Low-temperature specific heat and critical magnetic field of α-uranium single crystals

J. C. Lashley
Department of Chemistry and Biochemistry, Brigham Young University, Provo, Utah 84602
and Materials Science and Technology Division, Los Alamos National Laboratory, Los Alamos, New Mexico 87545

B. E. Lang, J. Boerio-Goates, and B. F. Woodfield
Department of Chemistry and Biochemistry, Brigham Young University, Provo, Utah 84602

G. M. Schmiedeshoff
Department of Physics, Occidental College, 1600 Campus Rd., Los Angeles, California 90041-3314

E. C. Gay and C. C. McPheeters
CMT Division, Argonne National Laboratory, Argonne, Illinois 60439

D. J. Thoma, W. L. Hults, J. C. Cooley, R. J. Hanrahan, Jr., and J. L. Smith
Materials Science and Technology Division, Los Alamos National Laboratory, Los Alamos, New Mexico 87545
(Received 28 November 2000; published 23 May 2001)

The current work reports on the specific heat and the electrical resistivity of α-uranium at cryogenic temperatures. Measurements were made on α-uranium single crystals that have some unexpected mechanical properties. Despite the fact that α-uranium normally work hardens and often fails in a brittle manner, these crystals bend easily. Presumably, the combination of flexibility and strength comes from twinning in response to stress, and these twins can run freely during deformation. Because grain boundaries are not present, we anticipated that the characteristics of the charge density wave (CDW) might be more prominent in these crystals. For these reasons, the specific heat was measured from $T \approx 0.5$ to 110 K, using semiadiabatic calorimetry in zero field, and the electrical resistivity was measured from $T \approx 0.1$ to 0.50 K, in magnetic fields up to 80 mT using a standard four-probe *ac* technique. An abrupt resistance drop typical of a superconducting transition was observed as the temperature fell below 0.78 K, a temperature at which the resistance fell to 90% from its original value. A residual resistivity ratio RRR$\approx$115 was measured from the low-temperature resistivity data. In addition, three phase transitions were clearly seen in the specific-heat data, located at $T = 23$, 36, and 42 K. These transitions are consistent with the α_3, α_2, and α_1 CDW structures that have been previously observed in uranium metal. Analysis of the specific-heat data give an electronic specific heat (γ) $= 9.13\ \mathrm{mJ\,K^{-2}\,mol^{-1}}$ and a low-temperature limiting Debye temperature (Θ_D) $= 256\ \mathrm{K}\ (\pm 0.25\ \mathrm{K})$. The highest calorimetric value measured previously was 218 K. Our value of 256 K is in favorable agreement with that previously obtained from elastic constants 250 K (± 2 K). The agreement between calorimetric and elastic Θ_D values, ductility at room temperature, and a RRR that is three times larger than previously reported values highlight the properties of these α-uranium single crystals.

DOI: 10.1103/PhysRevB.63.224510 PACS number(s): 74.70.Ad, 75.40.−s, 05.70.Fh, 05.70.Jk

I. INTRODUCTION

Although uranium is a fundamental element to nuclear physics, it exhibits extraordinary solid-state properties.[1] Knowledge of the solid-state properties has benefited from fifty years of metallurgical research aimed at nuclear fuel production. The solid-state properties include a series of three low-temperature charge density wave (CDW) structural phase changes in the normal state and a superconducting transition below 2 K that shows a large positive isotope effect when the CDW is suppressed by 11 kbar of pressure.[2,3] The superconducting transition in uranium is unique because it was the first example of a metal that becomes a superconductor under pressure without a crystallographic transition.[4] Additionally, superconductivity in uranium raised the important problem of bulk versus filamentary superconductivity for the first time.[1] In the normal state, the first CDW transition occurs at 43 K (α_1), the second at 38 K (α_2), and the last at 22 K (α_3), where the subscripts 1, 2, and 3 refer to the zero-pressure equilibrium phases. The α_1 transition is known to be the onset of the CDW state and is associated with a lattice distortion. Below 23 K, all three components of the CDW structure are commensurate with the underlying lattice, while the CDW structure becomes incommensurate with the underlying lattice between 23 and 43 K.[1,5] There is also a significant increase in the unit cell volume at the α_3 transition.[1]

For the reasons mentioned above, uranium has been the subject of many calorimetric investigations of both polycrystalline and single-crystal samples.[6–13] The resulting electronic specific heat (γ) and low-temperature limiting Θ_D parameters obtained from these studies are reported in Table I. After fifty years of multidisciplinary research, one might think that we could simply catalog the engineering properties of uranium and use this to know, for example, how to predict T_c. However, years of research have shown that T_c depends

TABLE I. Values of the electronic specific heat γ, Debye temperatures Θ_D, and T_c values reported by different investigators.

Investigators (Ref.)	γ (mJ K^{-2} mol^{-1})	Θ_D (K)	T_c (K)	Sample
Goodman and Schoenberg 1950 (Ref. 6)	10.6	206		Polycrystalline
Smith and Wolcott 1955 (Ref. 7)	10.9	200		Polycrystalline
Dempesy, Gordon, and Romer 1963 (Ref. 8)	12.1			Polycrystalline
Gordon *et al.* 1966 (Ref. 9)	10.12	183		Polycrystalline
	10.03	207		
Flotow and Osborne 1966 (Ref. 10)	9.88	218		Polycrystalline
Ho *et al.* 1966 (Ref. 4)	10.3[a]		<0.1	Pseudocrystal[c]
	12.2[b]		2.0	Polycrystalline
Fisher and Dever 1968[d] (Ref. 11)		250		Single crystal
Crangle and Temporal 1973 (Ref. 12)	10.00	195		Polycrystalline
	9.46	203		Large-grained
	9.14	210		Pseudocrystal
Bader, Phillips, and Fisher 1975 (Ref. 13)	9.59		0.27	Polycrystalline
	9.86		0.20	Polycrystalline
	9.82		0.27	Large-grained
	9.9		0.27	Large-grained
	9.14		<0.1	Single crystal
Current study	9.13	256		Single crystal

[a]Measurement done at 0.1 MPa.
[b]Measurement done at 1 GPa.
[c]Pseudocrystal is a term used to indicate the presence of substructure such as low angle grain boundaries in a crystal.
[d]Elastic constant measurements.

too sensitively on things such as impurities, temperature, and method of fabrication to be predictable. Accordingly, many ambiguities associated with the experimental situation and differing values summarized in Table I have been attributed to the purity of samples and the quality of single crystals. For example, calorimetric measurements made at 10 kbar are consistent with magnetic measurements and have confirmed the presence of bulk superconductivity with a T_c of 2 K,[14] and calorimetric measurements at zero pressure give widely different values for T_c ranging from 0.1 to 0.5 K, taking the midpoint of the rise in the C/T data. One model to explain this variation has been that certain impurities and/or filaments of strained material can help stabilize a bulk superconductor by suppression of the CDW.[15] In particular, it has been reported that a T_c between 0.25 and 0.80 K is due to strain filaments within the metal.[16] The values of the electronic specific heat and the Debye temperatures in the low-temperature limit appear to be influenced by the substructure within a crystal. The differences in the Debye temperatures have been ascribed to variations in the CDW suppression.[1] As noted in Table I, the values prior to the current study determined from C/T vs T^2 plots between 0 and 4 K, vary from 183 to 218 K. One can see that these values tend to be lower for polycrystalline samples.

The only Θ_D values for single crystal α-U that had previously been reported is that for a pseudo-single-crystal made by slow cooling from β-U to α-U by mechanically moving a sample through a temperature gradient. The calorimetric values were obtained and reported by Crangle and Temporal,[12] but the samples were made from experiments at Argonne. The microstructures and diffraction patterns showed considerable splitting of the alpha grains to produce mosaic boundaries between small grains that vary in orientation by as much as 15°. In contrast, the single crystals produced by a grain coarsening method are free of mosaic boundaries and have been used only to detect the T_c with calorimetric data between 0.1 and 1 K.[1] There is, therefore, no reported Θ_D for single crystals produced by grain coarsening, since the data reported in the review article by Lander *et al.*[1] represented C/T versus T data, with the T^{-3} and T^{-2} contributions removed. The calorimetric Θ_D of grain coarsened single-crystal α-U is still to be measured.

Recently, we prepared single crystals of α-uranium metal using electrochemical techniques. Although orthorhombic α-uranium normally work hardens rapidly and often fails in a brittle manner, these crystals bend easily and do not work harden. They were grown by electrotransport through a molten salt bath formed as dendrites.[17] These samples differ from samples used in previous investigations in that they are relatively strain free and show facets. It was anticipated that the characteristics of the low-temperature properties of uranium might be more prominent in these crystals because defects that typically pin the CDW state are not present. Although α-uranium has been the subject of numerous resistivity and calorimetric investigations, we were motivated to revisit the low-temperature physics of uranium with

these high-quality single crystals. The electrical resistance measurements reported here were undertaken to clarify the nature of superconductivity in single crystal α-uranium at zero pressure and to measure the critical magnetic field. The specific-heat measurements were undertaken to search for superconductivity at zero pressure and to obtain the thermodynamic properties of the CDW state. In addition, we investigate the 16% difference between the Debye temperatures previously obtained from specific heat data and those calculated from single-crystal elasticity measurements.

II. EXPERIMENT

A. Samples

The uranium crystals were grown by electrotransport through a molten salt bath of LiCl-KCl eutectic containing on the order of 3 wt. % UCl_3.[18] The uranium was deposited onto a stainless steel cathode as dendrites in the form of parallelogram-edged platelets, often diamond shaped. These individual platelets within the dendrites are single crystals of α-uranium. Because the uranium was deposited at temperatures below the α-β transformation temperature, they are strain free and nearly perfect. The crystals were characterized by a back-reflection Laue technique that determined that the *c* axis was orthogonal to the plate. Earlier investigations on bicrystal samples grown using a similar technique determined that the growth direction was $\langle 310 \rangle$. Parallelepiped strips and short cylindrical samples were shaped by spark-erosion cutting, and were cleaned in concentrated HNO_3 and electropolished in H_3PO_4.

B. Electrical resistivity

The electrical resistivity was measured using a standard four-probe ac technique. The magnetic field and current were parallel and perpendicular to the *c* axis, respectively. A Linear Research LR-700 resistance bridge, which implemented a standard four-terminal ac measurement at 16 Hz, was used in this measurement. The small resistance of the crystal (about 12 $\mu\Omega$) below 2 K required a large excitation current of 1.5 mA. The electrical resistance above 2 K was measured using a standard four-terminal ac technique with an excitation current of 3 mA. The resistivity was calculated from the dimension of the sample with an estimated absolute uncertainty of 15%.

C. Specific heat

The specific heat was measured in zero-magnetic field using an apparatus designed around a ^{3}He insert capable of attaining temperatures as low as 0.4 K. Two single crystals of uranium, weighing a total of 0.5 g, were stacked and thermally attached to the sample platform with a thin layer of Apiezon N grease. The specific heat of the empty sample platform was measured separately, and the specific heat of the empty sample platform and the Apiezon N grease was subtracted from the total specific heat to obtain the specific heat of the sample. A semiadiabatic pulse technique was used to measure the specific heat from the lowest temperature up to 10 K, and this technique was also used to map the α_3 transition. Semiadiabatic conditions are obtained by adding enough heat to obtain a flat drift at each temperature. An isothermal technique was used to measure the specific heat from 10 to 110 K. In the isothermal technique, a constant temperature block is heated to a series of predetermined temperatures and the sample is allowed to drift toward the block temperature before and after a heating pulse. The details of the semiadiabatic pulse and isothermal techniques and thermometry are described elsewhere.[19,20]

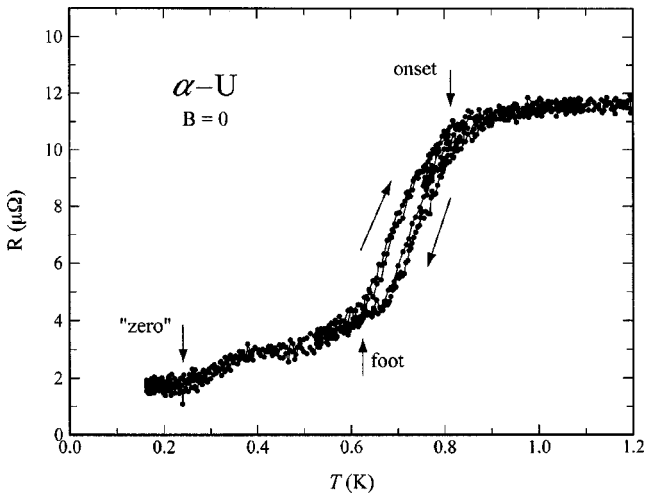

FIG. 1. Graphical definition of terms used in describing the resistivity data. We base the T_c on the foot value.

III. RESULTS AND DISCUSSION

A. Electrical resistivity

We observed an abrupt drop in the resistance of the crystal as the temperature fell below about 0.78 K, the temperature at which the resistance appears to reach its minimum value. The quantities are graphically defined in Fig. 1. The critical temperature, T_c, is taken to be the temperature at

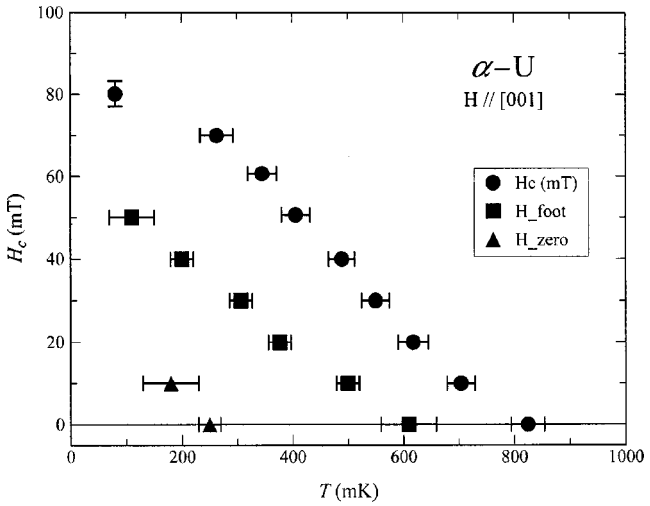

FIG. 2. Electrical resistivity data showing an abrupt resistance drop in the ''foot'' value at approximately 0.6 K. The magnetic field was parallel to the [001] direction in this experiment.

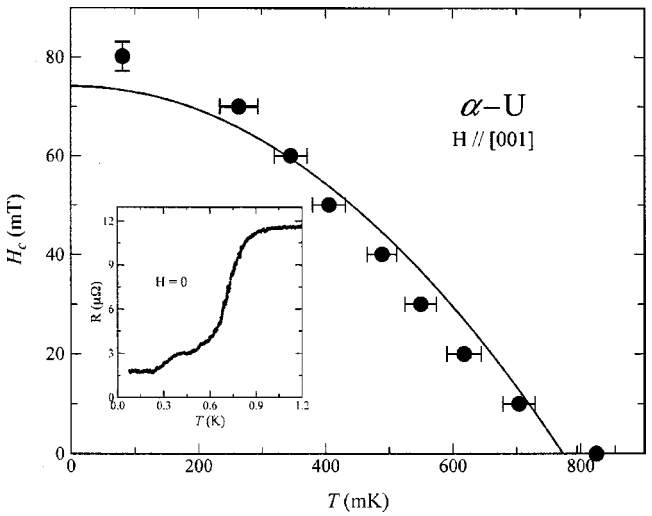

FIG. 3. A graph of $H_c(T)$ versus T. The $H_c(T)$ data evolves into quadratic temperature dependence in the low-temperature limit. Inset: The broad resistive transition arises from what we believe to be a small instrumental dc offset.

which the resistance falls to 90% of its value in the normal state. The dependence of T_c on H is shown in Fig. 2. These data are taken to mark the superconducting critical magnetic field H_c. The broad resistive transition, which is smoothed but is otherwise uncorrected for what we believe to be a small instrumental dc offset, is shown in the inset of Fig. 3. One can see a slight positive curvature just below T_c in the $H_c(T)$ data, which evolves into a quadratic temperature dependence as the temperature approaches 0 K. However, a fit of this data to Eq. (1) gives the qualitative form expected for type-I superconductors

$$H_c(T) = H_c(0)[1-(T/T_c)^2] \tag{1}$$

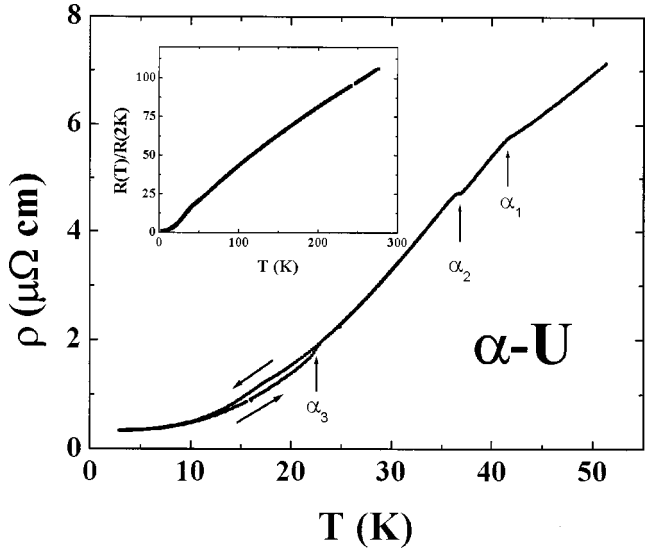

FIG. 4. The temperature dependence of the resistivity between $T \approx 2$ and 50 K. Diagonal arrows denote the direction in which the temperature was changing during data acquisition. Vertical arrows denote the position of the CDW features. Inset: The resistivity up to room temperature divided by its value near 2 K.

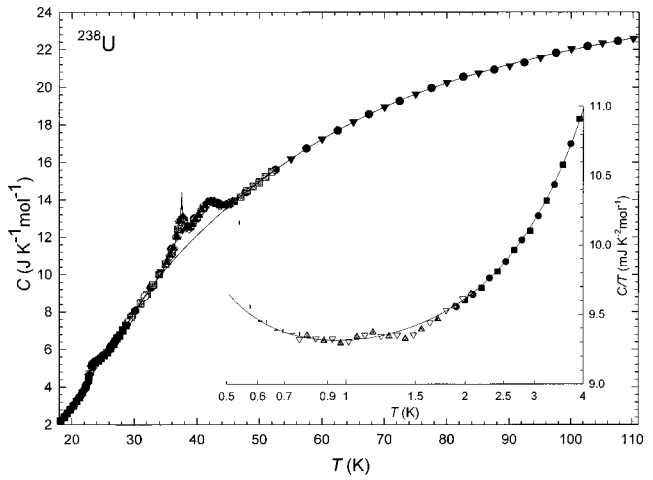

FIG. 5. The specific heat as a function of temperature is shown. Inset: The details of the specific heat below 4 K.

with $H_c(0) = 74 \pm 4$ mT and $T_c = 0.78 \pm 0.05$ K, shown as the solid line in Fig. 3, and characterizes the data reasonably well.

The temperature dependence of the resistivity between 2 and 50 K is shown in Fig. 4. Diagonal arrows denote the direction in which the temperature was changing during data acquisition. Vertical arrows denote the position of features we associate with the CDW transitions at $\alpha_1 = 42$ K, $\alpha_2 = 37$ K, and $\alpha_3 = 23$ K in good agreement with the values in the literature.[1] The inset shows the resistivity up to room temperature divided by its value near 2 K. Though similar in shape to earlier measurements reported in the literature,[1] our resistivity data is qualitatively different in that the features associated with all three CDW transitions are clearly visible: a break in slope at α_1, a steplike feature at α_2 (at which a small thermal hysteresis appears), and an abrupt onset of significant thermal hysteresis at α_3. The residual resistivity ratio (RRR) is about 115 which is three times higher than any RRR reported previously.[1] The magnetoresistance (with H parallel to the crystalline c axis) is very large and featureless, reaching approximately 750% at 18 T and at 2 K, a result which is also consistent with high-purity samples. A full description of our measurements in high magnetic fields will be reported elsewhere.

B. Specific heat

The specific heat of uranium, with four low-temperature anomalies, is shown in Fig. 5. As uranium cools to approximately 41 K, the α_1 appears as a round hump in the specific heat data. In contrast, the α_2 transition at approximately 38 K appears as a sharp peak. Further cooling of uranium to approximately 23 K results in yet another broad transition, the α_3 transition. Below 2 K there is a gradual upturn, typical of a ^{235}U hyperfine interaction, shown in the Fig. 5 inset. In order to calculate the excess specific heat from 10 to 110 K, the lattice specific heat was estimated by fitting the data using a hand spline.

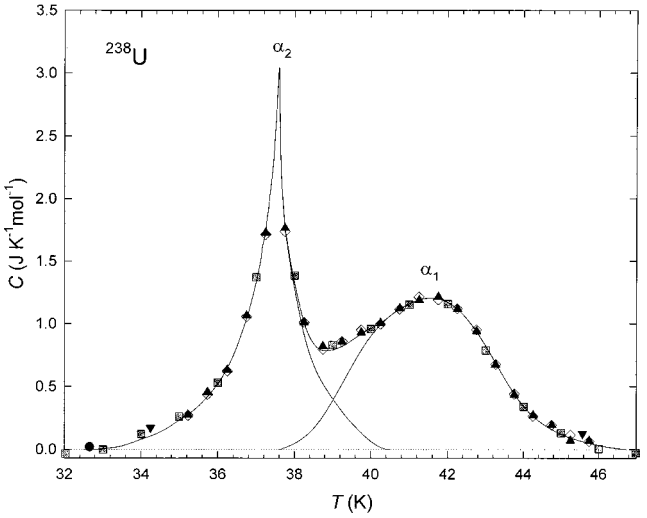

FIG. 6. The excess specific heat of the α_1 and α_2 CDW transitions. The lattice specific heat has been subtracted from the total specific heat in order to more clearly show the shape of these transitions.

1. The α_1 and α_2 transitions

Shown in Fig. 6 are the α_1 and α_2 transitions where a lattice estimation has been subtracted in order to more clearly show the excess specific heat of the transitions. The fit of each transition is extrapolated to the baseline to permit integration of each individual transition. In particular, α_2, which is clearly a symmetrical transition, was extrapolated to the high-temperature side and was then subtracted from the full transition (the lattice having already been subtracted) to obtain an estimate of the α_1 transition. We tested the self-consistency of our extrapolations by adding the two individual transitions, which resulted in the fit through the full transition as shown in Fig. 6. Integration of the C/T data gives an entropy of transition that is the same, within experimental error, for each phase change $\Delta S_{\alpha 1} = 0.12\ \mathrm{J\,K^{-1}\,mol^{-1}}$ and $\Delta S_{\alpha 2} = 0.11\ \mathrm{J\,K^{-1}\,mol^{-1}}$.

These transitions have been characterized as a structural and electronic transition at 41 K(α_1) accompanied by an electronic transition at 36 K(α_2).[1] The rounded symmetric shape of the α_1 transition is indicative of a sluggish first-order lattice transition, consistent with a change in the lattice parameter determined from prior neutron scattering experiments.[1] In contrast the α_2 transition at 38 K appears as a sharp peak which suggests there is very little lattice contribution at the α_2 transition. Several runs were made through this transition with decreasing ΔT intervals and are denoted by different data symbols in Fig. 6. Based on the sharp symmetric character of the α_2 transition and also on the presence of a transition in resistivity data at same temperature, we believe this transition is indicative of a first-order phase change. This observation is supported by recent first principles total energy calculations on the CDW state the results of which suggest that the α_2 transition is a modified α_1 CDW state caused by directional nesting of the Fermi surface.[21]

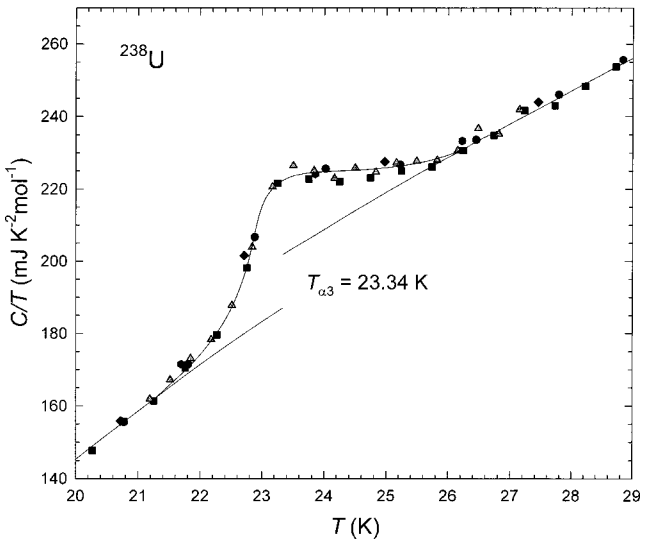

FIG. 7. The α_3 CDW transition is shown on an expanded scale. There is a obvious step in the lattice at this transition.

2. The α_3 transition

From 18 to 26 K an estimate of the lattice specific heat was interpolated through the α_3 transition at 23 K and is shown in Fig. 7. A baseline could not be drawn from the low-temperature to the high-temperature side of the transition without a discontinuous change. This obvious step in the baseline is consistent with a significant lattice coupling associated with the α_3 transition. To confirm this result, the specific heat was measured after cooling quickly through the transition, and the resulting specific heat data show an almost completely quenched transition. However, for slow cooling, the transition appears as a rise in the specific heat with a rounded transition. Despite the round shape of the transition, the presence of the step change in the baseline is strong evidence for a first-order phase change. Figure 8 illustrates the shape of the transition and the discontinuous baseline in the excess specific heat. The abrupt drop in the transition, as

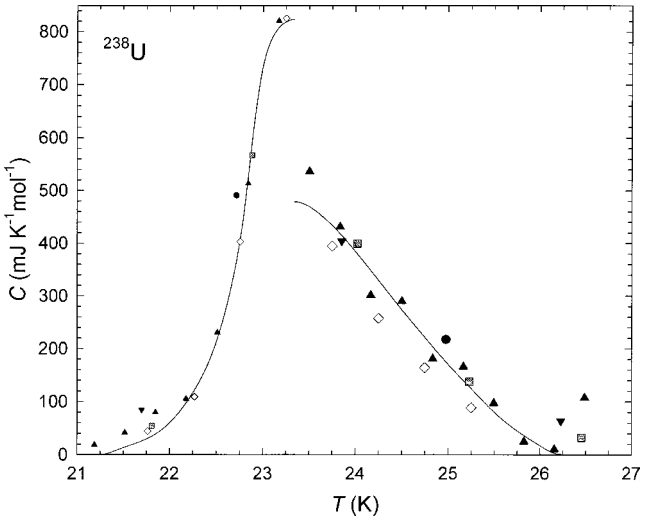

FIG. 8. The excess specific heat of the α_3 CDW transition is shown. One can see the effect of the discontinuous baseline.

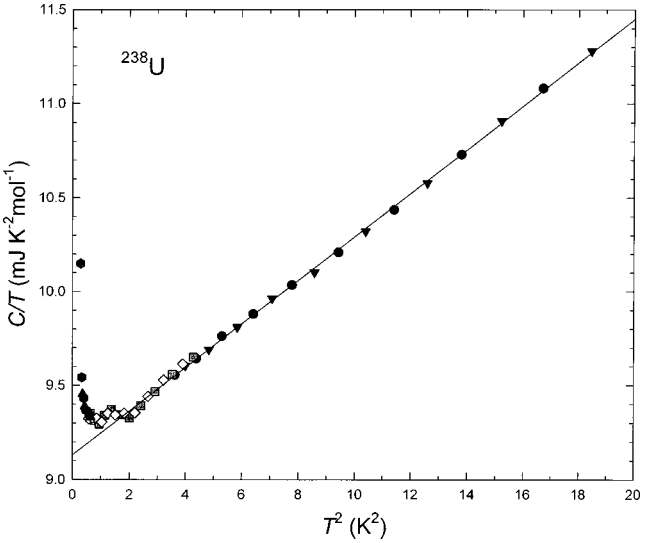

FIG. 9. The fit of the low-temperature specific heat data to Eq. (2) is shown.

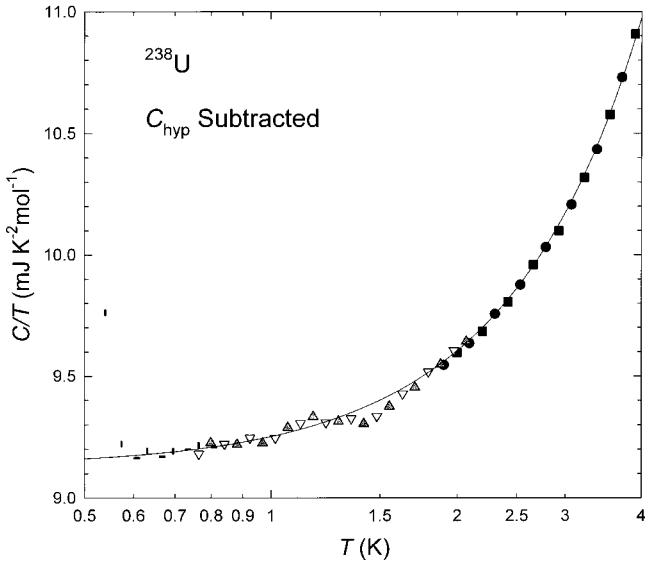

FIG. 10. The low-temperature specific heat is shown without the nuclear specific heat contribution. The nuclear specific heat, arising from nuclear spin from the ^{235}U isotope, was fit to Eq. (4) and subtracted from the total specific heat. The appearance of the oscillation at 1.2 K, although not entirely understood, it is not an artifact of our temperature scale.

seen in Fig. 8, is an artifact of the baseline offset. Presumably, if the transition were sharp, as would be the case for an ideally first-order transition, the abrupt baseline change would be absent. Integration of the C/T data yields an entropy of transition $\Delta S_{\alpha 3}=0.05\ \mathrm{J\,K^{-1}\,mol^{-1}}$, an entropy that is half of the two higher-temperature transitions.

3. T<10 K

The heat liberated from the depleted ^{238}U sample during its α-decay process prevented cooling to temperatures below 0.5 K in the specific-heat measurements. The electronic term (γ) and the Debye temperature (Θ_D) were obtained from a fit from 1.2 to 4 K using a conventional C/T versus T^2 extrapolation represented by Eq. (2), and is shown in Fig. 9

$$C/T=\gamma+B_3T^2. \tag{2}$$

A Debye temperature of 256 K ($\pm$0.25 K) and an electronic specific heat of 9.13 mJ K^{-2} mol^{-1} was also obtained from this fit. The lattice specific heat was fitted over a more extended temperature range from 1.2 to 10 K using the low-temperature expansion of the Debye function represented by Eq. (3)

$$C_V=\gamma T+B_3T^3+B_5T^5+B_7T^7+B_9T^9+B_{11}T^{11}+B_{13}T^{13}, \tag{3}$$

where the γ and B_3 terms were fixed at the values obtained from the C/T extrapolation, and the required number of adjustable parameters for the lattice (B_n) increased until a suitable fit was obtained. The importance of the expression with adjustable coefficients is that that is the form required for a lattice with harmonic forces, and large harmonic softening of the phonon density of states for α-U has been recently measured by inelastic neutron scattering.[22]

One can see a gradual upturn in the low-temperature C vs T data as shown in the inset of Fig. 5. This upturn is the nuclear specific heat and arises from the ^{235}U hyperfine interaction. This hyperfine interaction manifests itself as a nuclear Schottky anomaly, which has a T^{-2} temperature dependence in the high-temperature limit. The nuclear specific heat was fitted to the expression

$$C=\gamma T+B_3T^3+AT^{-2}, \tag{4}$$

where γ and B_3 were fixed at the values obtained from the fit to Eq. (2) and is shown as the line through the data in the inset of Fig. 5. A ^{235}U concentration of 0.58 at. % was estimated for our sample using the A term obtained from the fit and correlations of the hyperfine term to ^{235}U concentrations reported previously in the literature.[4] The ^{235}U hyperfine contribution C_{hyp} was subtracted from the specific heat data and the resulting fit to the data is shown in Fig. 10. The origin of the small oscillation in our specific heat data near 1.2 K remains unknown; however based on previous measurements, this oscillation it is not an artifact of our temperature scale.[19]

IV. CONCLUSION

An abrupt drop in the resistivity was observed at 0.78 K ($\pm$0.05 K) and a critical field $H_c(0)=74$ mT ($\pm$4 mT) was obtained from the low-temperature electrical resistivity measurements. The resistivity data for the superconducting transition fits the qualitative form expected for a type-I superconductor. Our electronic specific heat value ($\gamma=9.13\ \mathrm{mJ\,K^{-2}\,mol^{-1}}$) is within experimental error with the value previously reported by Bader *et al.*[13] and Crangle and Temporal.[12] In contrast, our Θ_D value of 256 K is higher than previously reported calorimetric values and agrees more closely with the value obtained from elastic constant measurements (250 K).[11]Agreement between Θ_D values and

from elastic constants and the thermal value indicate that the lattice appears to be strain free, a result that is substantially different than those obtained on single crystals grown by grain coarsening and perhaps explain the higher T_c. This result is confirmed by the measured RRR≈115 for these crystals.

The characteristics of the CDW appear to be more prominent in this sample as we observe transitions 1 K higher than previously measured. Despite the previous characterization of the α_1 transition as second order, we present evidence from a symmetrical-shaped transition that the α_1 transition is first order. The transition at 37 K shows clear first-order character and has a sharp peak in the excess specific heat. It is noteworthy that the entropies of the α_1 and α_2 transitions are equal, within experimental error. We also show evidence that the α_3 transition is first order and has a significant lattice component. The entropy of the α_3 transition is half that of the α_1 and α_2 transitions.

ACKNOWLEDGMENTS

We are grateful to Al Arko for review of this manuscript. We are indebted to Norman Phillips, Sam Bader, Ed Fisher, and Robert Fisher who did much of the pioneering work on the heat capacity of uranium. Part of this work was carried out at Brigham Young University and also at the Los Alamos National Laboratory supported under the Primary Physics Experiments Program, under the auspices of the Department of Energy. This work was partially supported by the National Science Foundation (NSF) under Grant No. DMR-0071947. The critical field and resistivity measurements were made at the National High Magnetic Field Laboratory, which is supported by NSF Cooperative Agreement No. DMR-9527035, and by the state of Florida.

[1] G. H. Lander, E. S. Fisher, and S. D. Bader, Adv. Phys. **43**, 1 (1994).
[2] E. S. Fisher and H. J. McSkimin, Phys. Rev. **124**, 67 (1961).
[3] R. D. Fowler, B. T. Matthias, L. P. Asprey, H. H. Hill, J. D. Lindsay, C. E. Olsen, and R. W. White, Phys. Rev. Lett. **19**, 892 (1967).
[4] J. C. Ho, N. E. Phillips, and T. F. Smith, Phys. Rev. Lett. **17**, 694 (1966).
[5] H. G. Smith, N. Wakacayashi, W. P. Crummett, R. M. Nicklow, G. H. Lander, and E. S. Fisher, Phys. Rev. Lett. **44**, 1612 (1980).
[6] B. B. Goodman and D. Schoenberg, Nature (London) **165**, 441 (1950).
[7] P. L. Smith and N. M. Wolcott, Suppl. Bull. l'Institut Friod (Paris) **1**, 283 (1955).
[8] C. W. Dempesy, J. E. Gordon, and R. H. Romer, Phys. Rev. Lett. **11**, 547 (1963).
[9] J. E. Gordon, H. Montgomery, R. J. Noer, S. Pickett, and R. Tobon, Phys. Rev. **152**, 432 (1966).
[10] H. E. Flotow and D. W. Osborne, Phys. Rev. **151**, 564 (1966).
[11] E. S. Fisher and D. Dever, Phys. Rev. **179**, 607 (1968).
[12] J. Crangle and J. Temporal, J. Phys. F: Met. Phys. **3**, 1097 (1973).
[13] S. D. Bader, N. E. Phillips, and E. S. Fisher, Phys. Rev. B **12**, 4929 (1975).
[14] C. W. Dempesy, J. E. Gordon, and R. H. Romer, Phys. Rev. Lett. **11**, 547 (1963).
[15] W. E. Gardner and T. F. Smith, Phys. Rev. **154**, 309 (1967).
[16] E. S. Fisher, T. H. Geballe, and J. M. Schreyer, J. Appl. Phys. **39**, 4478 (1968).
[17] H. F. McFarlane, K. M. Goff, F. S. Felicione, C. C. Dwight, and D. B. Barber, J. Met. **14**, 1 (1997).
[18] C. C. McPheeters, E. C. Gay, P. J. Karell, and J. P. Ackerman, J. Met. **49**, N7 (1997).
[19] B. F. Woodfield, Ph.D. thesis, University of California–Berkeley, 1995.
[20] J. C. Lashley, Ph.D. thesis, Brigham Young University, 2000.
[21] L. Fast, O. Eriksson, B. Johansson, J. M. Wills, G. Straub, H. Roeder, and L. Nördstrom, Phys. Rev. Lett. **81**, 2978 (1998).
[22] M. E. Manley, B. Fultz, R. J. McQueeney, C. M. Brown, W. L. Hults, J. L. Smith, D. J. Thoma, R. Osborn, and J. L. Robertson, Phys. Rev. Lett. **86**, 3076 (2001).